A g-factor metric for k-t SENSE and k-t PCA

Christian Binter[1], Rebecca Ramb[2], Bernd Jung[2], and Sebastian Kozerke[1,3]
[1]Institute for Biomedical Engineering, University and ETH Zurich, Zurich, Switzerland, [2]Dept. of Radiology, Medical Physics, University Medical Center, Freiburg, Germany, [3]Imaging Sciences and Biomedical Engineering, King's College London, London, United Kingdom

Purpose: Time resolved undersampling methods allow for a significant speed-up in image acquisition time by exploiting both spatial and temporal correlations of the data. However, the resulting noise enhancement not only varies spatially but is also strongly dependent on object dynamics. In addition, temporal low pass filtering may occur with increasing reduction factors. Both effects can be analyzed using pseudo-replica SNR measurements[1], which are, however, very time-consuming in terms of computational load. If frame-by-frame parallel imaging reconstruction is employed noise amplification is analytically described using the g-factor formalism[2,3]. In analogy, it is the purpose of the present work to propose a g-factor formulation for k-t undersampling methods including k-t SENSE and k-t PCA to assess spatiotemporal noise distributions and temporal fidelity of reconstructed signals.

Methods: For both k-t SENSE[4] and k-t PCA[5] the reconstruction matrix is given as $F = \theta E^H (E\theta E^H + \Psi)^{-1}$, where E denotes the encoding matrix, Ψ the receiver noise covariance matrix and Θ the signal covariance matrix calculated from the training data. Using the image noise matrix defined as $X = F\Psi F^H$ and the relationship $\sqrt{X_{xf}^{red}/X_{xf}^{full}} = g_{xf}\sqrt{R}$, the g-factor for a given spatial position x and frequency f can be expressed as:

$$g_{xf} = \sqrt{\underbrace{\left[\Theta E^H \left(E\Theta E^H + \Psi\right)^{-1} \Psi (E\Theta E^H + \Psi)^{-1} E\Theta^H\right]_{xf,xf}}_{\textit{main diagonal of undersampled image noise matrix } X^{red}/R} \underbrace{\left(E^H \Psi^{-1} E\right)_{xf,xf}}_{\textit{main diagonal of } X^{full}}}$$

For k-t PCA there are no distinct aliasing frequencies, therefore all n_{pc} principal components have to be stacked into the matrices, resulting in matrix sizes $[n_{coils}n_{freq} \times n_{pc}R]$ for E, $[n_{pc}R \times n_{pc}R]$ for Θ, and $[n_{coils}n_{freq} \times n_{coils}n_{freq}]$ for Ψ. In the case of k-t SENSE $n_{freq} = n_{pc}$.

A cine balanced SSFP scan of a short axis view was acquired in a healthy volunteer on a Philips Ingenia 3T scanner (Philips Healthcare, Best, The Netherlands) with a 12-channel coil array. Coil sensitivities were acquired using a separate scan. The overall SNR was set to 20, the local standard deviation of the noise was calculated using a pseudo-replica approach (250 repetitions). The temporal transfer function was determined by relating the magnitude in x-f domain obtained from undersampled data to the fully sampled dataset. All simulations were performed with 17 training profiles on a 336x336 matrix, resulting in effective reduction factors of 1.91, 3.5 and 6 for R=2, 4 and 8, respectively.

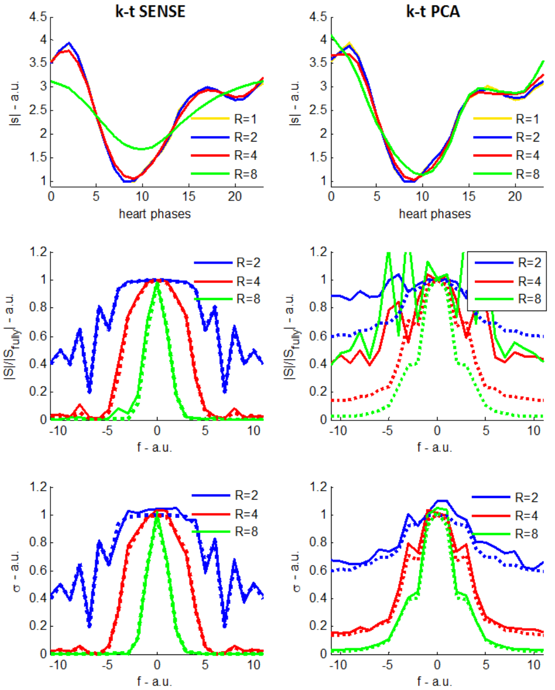

Fig. 1: Temporal fidelity and noise characteristics for different acceleration factors. Top row: Time course of signal magnitude. Middle: Corresponding transfer function in frequency domain. Bottom row: Noise standard deviation relative to fully sampled acquisition. The dotted lines are the calculated g_{xf}-factors. The location of the analyzed pixel is shown in Fig. 2.

Results: Fig. 1 compares the noise standard deviation as calculated using the pseudo-replica approach, and the g_{xf}-factor for all temporal frequencies. The noise standard deviations are scaled by $\sqrt{R}$. Fig. 2 shows example g_{xf}-factor maps for different reduction factors. With increasing reduction factor, decreasing values of g_{xf} at higher temporal frequencies are found while values at DC (f=0) vary only slightly (peak g_{xf} (f=0) were 1.05, 1.06, 1.08 for k-t PCA R=2, 4 and 8).

Discussion and Conclusion: The proposed g_{xf}-factor metric provides an analytical description of spatial and temporal noise behavior in k-t SENSE and k-t PCA. It can be seen that the regularization employed in k-t SENSE and k-t PCA yields g_{xf}-factor values mostly smaller than 1, especially at higher temporal frequencies indicating temporal low pass filtering. The results also show that the g_{xf} drop-off at higher frequencies increases with R, while values at DC increase only marginally. Accordingly, increasing reduction factors primarily affect temporal fidelity rather than noise level. For k-t SENSE the g_{xf}-factor directly approximates the temporal transfer function, providing a measure of both noise behavior and temporal filtering. In k-t PCA g_{xf}-factor metric and transfer function depart due to the temporal basis transformation involved as demonstrated (**Fig. 1**).

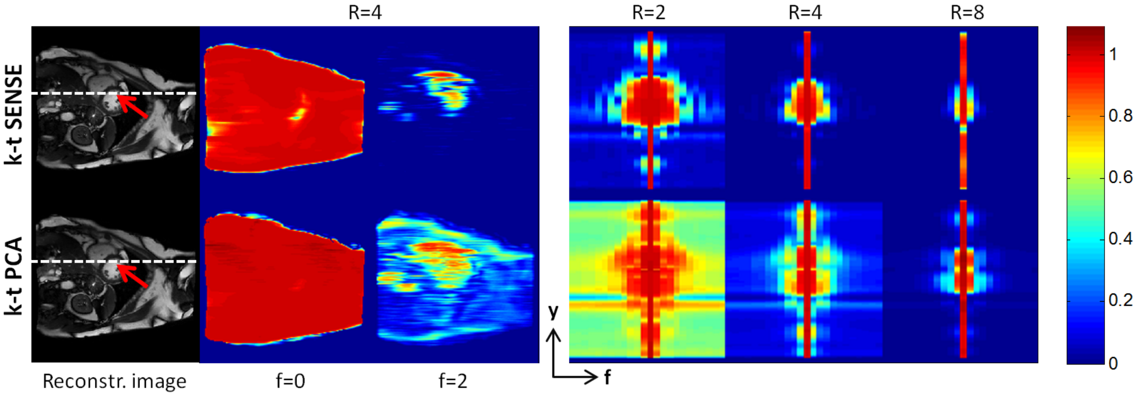

Fig. 2: g_{xf}-factor maps for k-t SENSE and k-t PCA at two different temporal frequencies (left), and g_{xf}-factors along the indicated dotted line for different acceleration factors (right). The arrow points to the pixel chosen for the plots in Fig. 1.

References: [1]Robson et al., Magn Reson Med 2008, 60(4): 895-907.
[2]Pruessmann et al., Magn Reson Med 1999, 42(5): 952-962.
[3]Breuer et al., Magn Reson Med 2009, 62(3): 739-746.
[4]Tsao et al., Magn Reson Med 2003, 50(5):1031-42.
[5]Pedersen et al., Magn Reson Med 2009, 62(3): 706-716.